Annals of Nuclear Medicine Vol. 21, No. 2, 101–107, 2007

Initial evaluation of dynamic human imaging using ^{18}F-FRP170 as a new PET tracer for imaging hypoxia

Tomohiro KANETA,*[1] Yoshihiro TAKAI,*[2] Ren IWATA,*[3] Takashi HAKAMATSUKA,*[1] Hiroyasu YASUDA,*[4] Katsutoshi NAKAYAMA,*[4] Yoichi ISHIKAWA,*[3] Shoichi WATANUKI,*[3] Shozo FURUMOTO,*[3] Yoshihito FUNAKI,*[3] Eiko NAKATA,*[2] Keiichi JINGU,*[5] Michihiko TSUJITANI,*[6] Masatoshi ITO,*[3] Hiroshi FUKUDA,*[7] Shoki TAKAHASHI*[1] and Shogo YAMADA*[5]

*[1]*Department of Diagnostic Radiology, Tohoku University*
*[2]*School of Health Sciences, Faculty of Medicine, Tohoku University*
*[3]*Cyclotron and Radioisotope Center, Tohoku University*
*[4]*Department of Geriatric and Respiratory Medicine, Tohoku University*
*[5]*Department of Radiation Oncology, Tohoku University*
*[6]*POLA Chemical Industries, Yokohama*
*[7]*Institute of Development, Aging and Cancer, Tohoku University*

^{18}F-FRP170, 1-(2-fluoro-1-[hydroxymethyl]ethoxy)methyl-2-nitroimidazole, is a new hypoxia imaging agent for positron emission tomography. This compound was synthesized by ^{18}F-labeling of RP170, which was developed as a new hydrophilic 2-nitroimidazole analog. In the present study, we analyzed dynamic whole-body imaging in healthy volunteers and dynamic tumor imaging in three patients with lung cancer. ***Methods:*** Four healthy male volunteers and three lung cancer patients were enrolled in this study. Volunteers underwent dynamic whole-body scans just after injection of ^{18}F-FRP170 for about 90 min, while the lung cancer patients underwent dynamic tumor imaging for about 60 or 120 min. Data are expressed as standardized uptake values (SUV). Regions of interest were placed over images of each organ or tumor to generate time-SUV curves. ***Results:*** The series of dynamic whole-body scans showed rapid elimination of ^{18}F-FRP170 from the kidneys following elimination from the liver. Very low physiological uptake was observed above the diaphragm. ^{18}F-FRP170 uptake in the lung cancer lesion could be visualized clearly from early after injection. The changes of tumor SUV, tumor/blood ratio, or tumor/muscle ratio about 30 min after injection or later were small. ***Conclusions:*** Dynamic imaging using ^{18}F-FRP170 demonstrated rapid elimination from the kidney, suggesting the high hydrophilicity of this imaging agent. The background activity above the diaphragm was very low, and patients with lung cancer showed clear tumor uptake of ^{18}F-FRP170 early after injection.

Key words: hypoxia, PET, nitroimidazole, RP170, FRP170

INTRODUCTION

THE 2-NITROIMIDAZOLE ANALOGS are known to have an interesting property, namely, they accumulate selectively in hypoxic tissue. The mechanism for the intracellular retention in hypoxic cells is not fully understood. It is believed that 2-nitroimidazoles undergo nitro-reduction with the formation of products that bind to intracellular elements and remain trapped in hypoxic tissues.[1] In 1981, it was suggested that radiolabeled 2-nitroimidazoles could be used for the direct visualization of tissue hypoxia in tumors.[2] ^{18}F-fluoromisonidazole (^{18}F-FMISO) was the first such radiopharmaceutical developed, and was used most widely for imaging hypoxia.[3,4] However, misonidazole is a rather lipophilic compound, and the images of

Received August 10, 2006, revision accepted November 30, 2006.

For reprint contact: Tomohiro Kaneta, M.D., Ph.D., Department of Diagnostic Radiology, Tohoku University, 1–1 Seiryomachi, Aoba-ku, Sendai 980–8574, JAPAN.
E-mail: kaneta@rad.med.tohoku.ac.jp

^{18}F-FMISO may have a low target-to-background ratio. Therefore, there is ongoing research to develop better compounds for clinical use. POLA Chemical Industries (Yokohama, Japan) have developed RP170, 1-(2-hydroxy-1-[hydroxymethyl]ethoxy)methyl-2-nitroimidazole, a new 2-nitroimidazole analog with hydrophilic side chain. The octanol-water partition coefficient (p value) of RP170 is 0.094, which was much lower than that of misonidazole (p value: 0.35–0.43), suggesting high hydrophilicity.[5–8] ^{18}F-FRP170, 1-(2-fluoro-1-[hydroxymethyl]ethoxy)methyl-2-nitroimidazole, is a fluorine-18 labeled compound of RP170 for use in clinical PET imaging, which is expected to show improvements over ^{18}F-FMISO with regard to higher image contrast and faster clearance.[9,10] In the present study, we performed whole-body imaging using ^{18}F-FRP170 in healthy volunteers, and evaluated the changes in the biodistribution of the tracer over time. Moreover, we performed dynamic tumor imaging in three patients with lung cancer, and evaluated the changes in tumor visualization over time.

MATERIALS AND METHODS

Radiosynthesis

^{18}F-FRP170 was prepared by nucleophilic ^{18}F-fluorination of the precursor, 1-[2-(toluene-4-sulfoxy)-1-(acetoxymethyl)ethoxy]methyl-2-nitroimidazole, followed by deprotection and HPLC purification. Radiochemically pure ^{18}F-FRP170 was obtained in overall yields of 3–11% (EOB: end of bombardment) with specific activity of >26 GBq/μmol (EOS: end of synthesis) within 90 min.[9]

Human subjects

This study was approved by the Ethics Committee of Tohoku University Hospital. Four healthy male volunteers aged 21, 23, 32, and 54 years and weighing 66.9, 58.0, 78.0, and 70.0 kg, respectively, and three lung cancer patients (Table 1) gave their written informed consent to participate in the study. The volunteers were free of medical illness as determined from their medical histories.

PET imaging procedure

During data acquisition, subjects were placed in the supine position with the arms alongside the body in the SET-2400W scanner (Shimadzu, Kyoto, Japan). This scanner consists of four rings of 112 BGO detector units (22.8 mm in-plane × 50 mm axial × 30 mm depth). Each detector unit has a 6 (in-plane) × 8 (axial) matrix of BGO crystals coupled to two dual photomultiplier tubes. They are arranged in 32 rings giving 63 two-dimensional image planes. Sensitivity for a 20-cm cylindrical phantom was 6.1 kcps/kBq/m*l* (224 kcps/microCi/m*l*) in 2D clinical mode.[11]

Transmission scans of each subject were obtained prior to injection of the tracer using ^{68}Ge retractable rods. Transmission scans lasted for 3 min per bed position (field of view, 20 cm), and these scans were used for subsequent attenuation correction of emission scans.

Dynamic whole-body emission scans for volunteers were performed for about 90 min after intravenous bolus injection of about 185 MBq of ^{18}F-FRP170 using 2-min step acquisition, with six steps for each scan from the head to the upper part of the thigh (2D acquisition mode). Dynamic tumor scans for patients were acquired for 120 min (case 1) or 60 min (cases 2 & 3). The frame rate was 15 × 2 min, and 18 (or 6) × 5 min.

PET data analysis

Organ activity concentration data were obtained by drawing regions of interest (ROIs) on the PET images for the brain, neck, thoracic aorta (blood), lung, heart, liver, spleen, gall bladder, kidney (renal cortex), and thigh (muscle) for volunteers, and for the tumor, thoracic wall (muscle), and thoracic aorta (blood) for the patients. Data are expressed as standardized uptake values (SUV), and time-SUV curves were obtained for all of these organs.

Table 1 Data for individual cases

Case no.	Age	Sex	Histologic type
1	79	M	SqCC
2	81	M	SqCC
3	71	F	Adeno

M: male, F: female, SqCC: squamous cell carcinoma, Adeno: adenocarcinoma

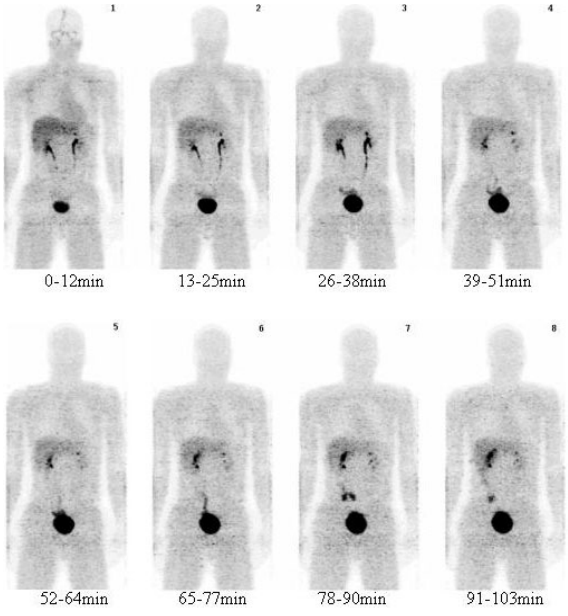

Fig. 1 A series of dynamic whole-body images of a 32-year-old male volunteer. Images are expressed as maximum intensity projections. Scans were performed head-first, and each scan took about 12 min.

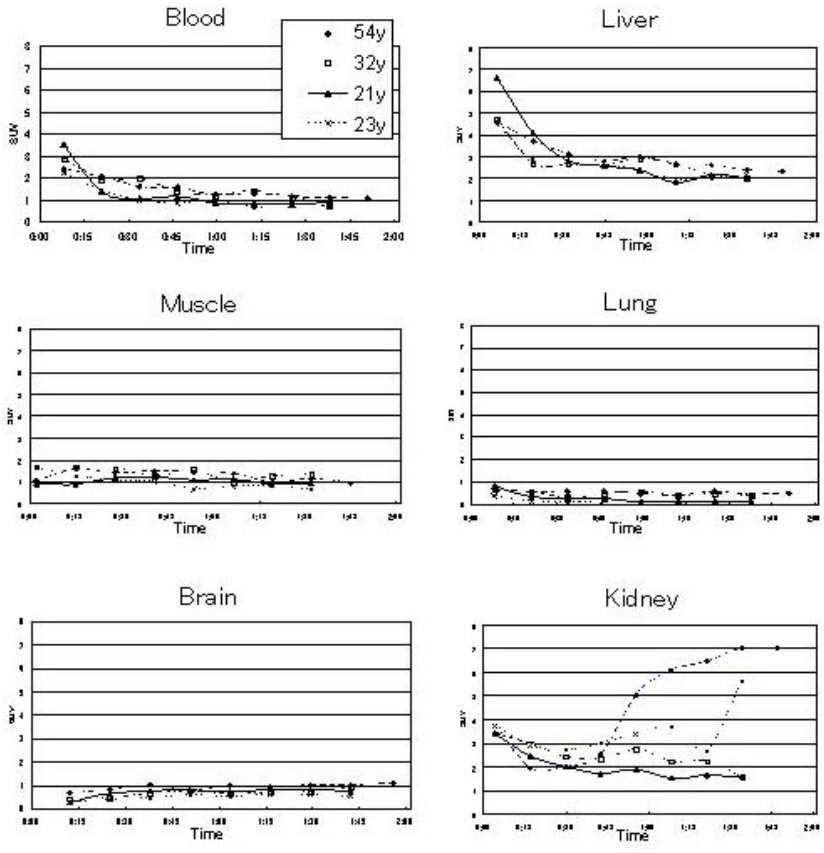

Fig. 2 SUV changes of the blood, liver, muscle, lung, brain, and kidneys of all four subjects. y = years-old

RESULTS

Studies in healthy volunteers

Dynamic whole-body imaging

Figure 1 shows a series of dynamic whole-body images (maximum intensity projection) of a 32-year-old male volunteer. In the first image obtained just after injection, strong levels of activity were seen in the bladder and ureter. The gall bladder and intestines were beginning to be visualized from the 6th image obtained about 1 h after injection.

Figure 2 shows the SUV changes of the blood, liver, muscle, lung, brain, and kidney in all four subjects. SUV was highest in the liver, followed by the kidney, while the lungs and brain showed very low SUV. Other organs showed moderately high SUV. With the exception of the brain, which showed an increase over time, almost all organs showed decreases in SUV over time.

Studies in patients

Figures 3, 4, and 5 show the results in cases 1, 2, and 3, respectively. All figures consist of CT images of the lung tumor, PET images at one hour after injection, the time-SUV curves of the tumor, muscle, and blood, and the time-ratio curves of tumor/muscle and tumor/blood.

Immediately after injection, SUV of the blood rose rapidly and showed a peak within 4 min. It showed a rapid decrease after the peak and progressed to a moderate decrease within 10 min. In cases 1 and 3, SUV of the blood dropped relative to that of tumor at around 30 min, but in case 2, SUV of the blood exceeded that of the tumor throughout the study period. SUV of muscle always showed the lowest value.

Figures 3D, 4D, and 5D show the changes in tumor/muscle and tumor/blood ratios. The tumor/muscle ratio showed a wide degree of variation early after injection, and increased slightly from about 45–60 min after injection. The tumor/blood ratio increased rapidly immediately after injection, and showed a slight increase from about 15 min after injection. The changes of these ratios about 30 min after injection or later were small.

Figure 6 shows tumor images of case 1 acquired from emission data for 10 min from 10–20 min, 30–40 min, 50–60 min, 70–80 min, 90–100 min, and 110–120 min after injection. Tumor uptake can be seen clearly on all of these images. The image contrast tended to increase with time, while the image quality decreased due to the radioactive decay of the tracer.

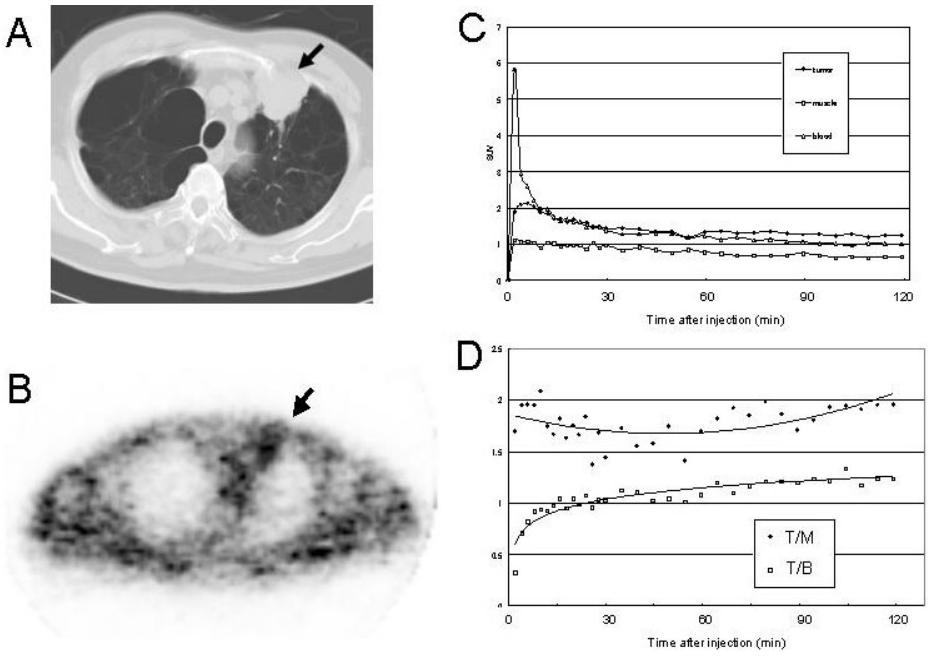

Fig. 3 Case 1: A 79-year-old male patient with lung squamous cell carcinoma. A: CT of the chest. A tumor was detected in the left upper lobe (*arrow*). B: ^{18}F-FRP170 PET image corresponding to the previous CT. Increased uptake (*arrow*) was seen corresponding to the lung tumor. C: Time-SUV curves of tumor (*closed diamonds*), muscle (*open squares*), and blood (*open triangles*). D: Time-ratio curves of tumor/muscle (T/M: *closed diamonds*) and tumor/blood (T/B: *open squares*). The solid lines for tumor/muscle ratio and tumor/blood ratio show the polynomial approximated curve and the log approximated curve, respectively.

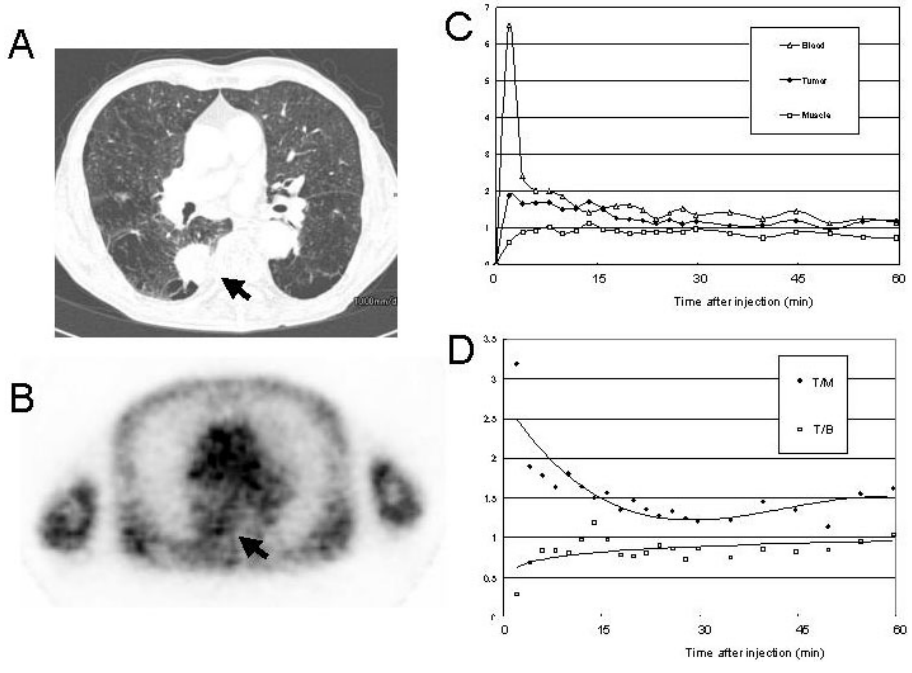

Fig. 4 Case 2: An 81-year-old male patient with lung squamous cell carcinoma. A: CT of the chest. A tumor was detected in the right lower lobe (*arrow*). B: ^{18}F-FRP170 PET image corresponding to the previous CT. Increased uptake (*arrow*) was observed corresponding to the lung tumor. C: Time-SUV curves of tumor, muscle, and blood. D: Time-ratio curves of tumor/muscle and tumor/blood.

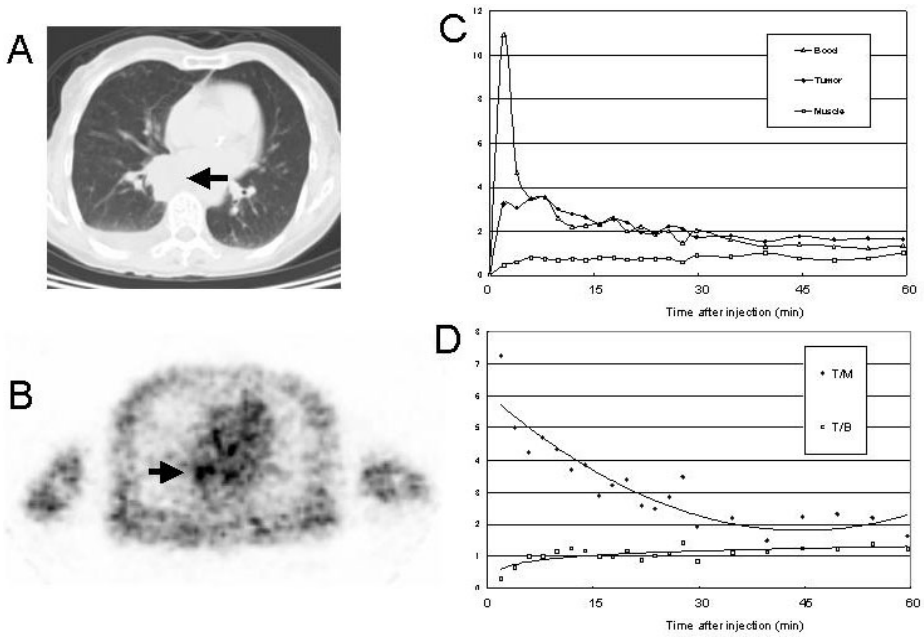

Fig. 5 Case 3: A 71-year-old female patient with lung adenocarcinoma. A: CT of the chest. A tumor was detected in the right lower lobe (*arrow*). B: ^{18}F-FRP170 PET image corresponding to the previous CT. Increased uptake (*arrow*) was observed corresponding to the lung tumor. C: Time-SUV curves of tumor, muscle, and blood. D: Time-ratio curves of tumor/muscle and tumor/blood.

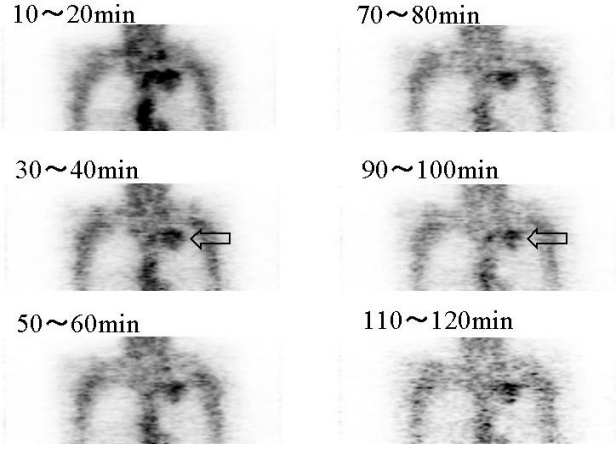

Fig. 6 Tumor images of case 1 acquired 10–20 min, 30–40 min, 50–60 min, 70–80 min, 90–100 min, and 110–120 min after injection. Tumor uptake was seen in the left upper lung (*open arrow*).

DISCUSSION

Since the 1990s, there have been many intensive studies using ^{18}F-FMISO, and a great deal of research effort has been directed toward synthesizing new hypoxia markers that overcome the limitations of ^{18}F-FMISO. Compounds characterized by high hydrophilicity were thought to be better for imaging hypoxia because of rapid blood clearance and high target-to-background ratio. Therefore, many 2-nitroimidazole analogs have been developed by changing the side chain of the drug. For example, etanidazole is a well-known hydrophilic 2-nitroimidazole analog with a p value of 0.046.[12] Even after fluorination, fluoroetanidazole (FETA) also showed a lower p value (0.16)[13] than FMISO (0.40).[8] It followed that the levels of retention of ^{18}F-FETA in the liver and lung were significantly lower than those of ^{18}F-FMISO.[14] More recently, ^{18}F-fluoroerythronitroimidazole (^{18}F-FETNIM) and ^{18}F-fluoroazomycin arabinoside (^{18}F-FAZA) have been developed as hydrophilic hypoxia markers. The p value of ^{18}F-FETNIM was reported to be 0.17, and the tumor-to-blood ratio with ^{18}F-FETNIM at 4 h after injection was significantly higher than with ^{18}F-FMISO.[8] Kumar et al. reported that p values of ^{18}F-FAZA and ^{18}F-FMISO were 1.1 and 2.6, respectively.[15] They reported that ^{18}F-FAZA displays a lower p value than ^{18}F-FMISO, indicating the potential for both rapid diffusion through tissue and faster renal excretion. In fact, ^{18}F-FAZA produced higher target-to-background ratios compared with ^{18}F-FMISO.[16] From these results, ^{18}F-FRP170 is also expected to yield images with high contrast and a low background level. By comparison with clinical images using ^{18}F-FMISO[17] or ^{18}F-FETNIM,[18] the images of ^{18}F-FRP170 seem to be almost equivalent to those of these tracers, even acquired 1 h after injection. However, it is difficult to discuss the differences in the images precisely without direct comparison in matched patients and with matched protocols.

In mice, the highest and second highest absorbed doses of ^{18}F-FRP170 were seen in the liver and kidney respectively.[19] The estimated average whole-body absorbed

dose for humans is 4.5 μGy/MBq, and the estimated effective doses for men and women are 5.4 μSv/MBq and 5.7 μSv/MBq, respectively. These observations suggest that an injected dose of 185 MBq of ^{18}F-FRP170 is safe for clinical use.

In the volunteer study, ^{18}F-FRP170 showed rapid elimination from almost all organs *via* excretion through the urinary pathway. In addition, its excretion into the bile was delayed. These observations were thought to be due to the high degree of hydrophilicity of the tracer. In addition, our results demonstrated that ^{18}F-FRP170 uptake in the brain was low, but increased gradually over time. Misonidazole, which is a representative 2-nitroimidazole is known to induce peripheral neuropathy after exceeding a schedule-dependent cumulative threshold dose.[20] This observation along with our results suggests the cumulative tendency of 2-nitroimidazoles in the brain.

Clinical PET scan using ^{18}F-FMISO is generally performed about 2 h or more after injection.[4,19,21] However, the strongly hydrophilic character of ^{18}F-FRP170 means that the ^{18}F-FRP170 PET scan can be started less than 2 h after injection. Moreover, due to the very low levels of physiological uptake above the diaphragm, we expected good tumor/background contrast in the lungs, mediastinum, head & neck, and brain.

In accordance with these results, we performed initial tumor imaging using ^{18}F-FRP170 in patients with lung cancer. Based on the results of our volunteer studies, lung cancer was expected to show good contrast images with low background levels. In fact, ^{18}F-FRP170 uptake in the lung cancer could be visualized clearly from early after injection. The tumor/muscle ratio tended to decrease slightly prior to 45–60 min after injection, but then tended to increase slightly. On the other hand, the tumor/blood ratio showed a rapid increase prior to about 30 min after injection, after which it increased gradually with time. The tumor/muscle ratio and tumor/blood ratio in case 1 were 1.69 and 1.09 at 1 h after injection, and 1.96 and 1.24 at 2 h, respectively. Both the tumor/muscle and tumor/blood ratios were higher 2 h than 1 h after injection, although the differences were too small to detect visually. The images obtained about 60 min after injection may be of sufficient quality to allow evaluation of tumor uptake in a clinical setting. However, considering the recent advances of PET technology, the images of ^{18}F-FRP170 demonstrated in the present study may have room for improvement. For example, increasing injected doses, longer emission-scan time, or using the latest PET/CT scanner may improve the image quality. The 2-nitroimidazoles are known to enter the cells by passive diffusion; therefore, their intracellular uptake is thought not to be particularly high. It may be necessary to administer a larger amount of radioactivity than that used in the present study. From the standpoint of estimated radiation dose,[19] about 370–555 MBq of ^{18}F-FRP170 may be considered safe for use in adults.

In this study, we did not perform direct determination of oxygen tension of the tumor or immunohistochemical detection of oxygen-dependent gene expression. Therefore, we cannot discuss the relationship between the degree of tumor hypoxia and the tumor uptake of ^{18}F-FRP170 in the present study. Further investigations are required to clarify this issue.

CONCLUSIONS

We analyzed dynamic ^{18}F-FRP170 images obtained in healthy volunteers and in three patients with lung cancer. Rapid elimination of the tracer from the kidney was seen in the volunteers, supporting the strong hydrophilicity of ^{18}F-FRP170. The images obtained in the cases of the lung cancer patients demonstrated good image contrast even at 1 h after injection. ^{18}F-FRP170 could be expected to yield good tumor images and allow scanning to begin early, but further investigations are warranted to clarify these points.

ACKNOWLEDGMENTS

This work was supported by the Grant-in-Aid for Scientific Research (10470191, 17659361) from the Ministry of Education, Science and Culture of Japan, and the Grant-in-Aid for Cancer Research (17-12) from the Ministry of Health, Labour and Welfare of Japan.

REFERENCES

1. Nunn A, Linder K, Strauss HW. Nitroimidazoles and imaging hypoxia. *Eur J Nucl Med* 1995; 22: 265–280.
2. Chapman JD, Franko AJ, Sharplin J. A marker for hypoxic cells in tumours with potential clinical applicability. *Br J Cancer* 1981; 43: 546–550.
3. Koh WJ, Bergman KS, Rasey JS, Peterson LM, Evans ML, Graham MM, et al. Evaluation of oxygenation status during fractionated radiotherapy in human nonsmall cell lung cancers using [F-18]fluoromisonidazole positron emission tomography. *Int J Radiat Oncol Biol Phys* 1995; 33: 391–398.
4. Rasey JS, Koh WJ, Evans ML, Peterson LM, Lewellen TK, Graham MM, et al. Quantifying regional hypoxia in human tumors with positron emission tomography of [^{18}F]fluoromisonidazole: a pretherapy study of 37 patients. *Int J Radiat Oncol Biol Phys* 1996; 36: 417–428.
5. Sasai K, Shibamoto Y, Takahashi M, Abe M, Wang J, Zhou L, et al. A new, potent 2-nitroimidazole nucleoside hypoxic cell radiosensitizer, RP170. *Jpn J Cancer Res* 1989; 80: 1113–1118.
6. Murayama C, Suzuki A, Sato C, Tanabe Y, Miyata Y, Shoji T, et al. Radiosensitization by 2-nitroimidazole nucleoside analog RP-170: radiosensitizing effects under both intravenous and oral administration. *Int J Radiat Oncol Biol Phys* 1992; 22: 557–560.
7. Murayama C, Suzuki A, Suzuki T, Miyata Y, Sakaguchi M, Tanabe Y, et al. Radiosensitization by a new nucleoside analogue: 1-[2-hydroxy-1-(hydroxymethyl)ethoxy]methyl-

2-nitroimidazole (RP-170). *Int J Radiat Oncol Biol Phys* 1989; 17: 575–581.
8. Yang DJ, Wallace S, Cherif A, Li C, Gretzer MB, Kim EE, et al. Development of F-18-labeled fluoroerythronitroimidazole as a PET agent for imaging tumor hypoxia. *Radiology* 1995; 194: 795–800.
9. Wada H, Iwata R, Ido T, Takai Y. Synthesis of 1-[2-[^{18}F]fluoro-1-(hydroxymethyl)-ethoxy]methyl-2-nitroimidazole ([^{18}F]FENI), a potential agent for imaging hypoxic tissues by PET. *J Label Compd Radiopharm* 2000; 43: 785–793.
10. Kaneta T, Takai Y, Kagaya Y, Yamane Y, Wada H, Yuki M, et al. Imaging of ischemic but viable myocardium using a new ^{18}F-labeled 2-nitroimidazole analog, ^{18}F-FRP170. *J Nucl Med* 2002; 43: 109–116.
11. Fujiwara T, Watanuki S, Yamamoto S, Miyake M, Seo S, Itoh M, et al. Performance evaluation of a large axial field-of-view PET scanner: SET-2400W. *Ann Nucl Med* 1997; 11: 307–313.
12. Brown JM, Workman P. Partition coefficient as a guide to the development of radiosensitizers which are less toxic than misonidazole. *Radiat Res* 1980; 82: 171–190.
13. Barthel H, Wilson H, Collingridge DR, Brown G, Osman S, Luthra SK, et al. *In vivo* evaluation of [^{18}F]fluoroetanidazole as a new marker for imaging tumour hypoxia with positron emission tomography. *Br J Cancer* 2004; 90: 2232–2242.
14. Rasey JS, Hofstrand PD, Chin LK, Tewson TJ. Characterization of [^{18}F]fluoroetanidazole, a new radiopharmaceutical for detecting tumor hypoxia. *J Nucl Med* 1999; 40: 1072–1079.
15. Kumar P, Stypinski D, Xia H, McEwan A, Machulla H, Wiebe LI. Fluoroazomycin arabinoside (FAZA): Synthesis, ^{2}H and ^{3}H-labelling and preliminary biological evaluation of a novel 2-nitroimidazole marker of tissue hypoxia. *J Label Compd Radiopharm* 1999; 42: 3–16.
16. Piert M, Machulla HJ, Picchio M, Reischl G, Ziegler S, Kumar P, et al. Hypoxia-specific tumor imaging with ^{18}F-fluoroazomycin arabinoside. *J Nucl Med* 2005; 46: 106–113.
17. Eschmann SM, Paulsen F, Reimold M, Dittmann H, Welz S, Reischl G, et al. Prognostic impact of hypoxia imaging with ^{18}F-misonidazole PET in non-small cell lung cancer and head and neck cancer before radiotherapy. *J Nucl Med* 2005; 46: 253–260.
18. Lehtio K, Eskola O, Viljanen T, Oikonen V, Gronroos T, Sillanmaki L, et al. Imaging perfusion and hypoxia with PET to predict radiotherapy response in head-and-neck cancer. *Int J Radiat Oncol Biol Phys* 2004; 59: 971–982.
19. Ishikawa Y, Funaki Y, Iwata R, Furumoto S, Nakata E, Kudo Y, et al. [Development of [^{18}F]FRP-170 injection for imaging hypoxia by PET]. *KAKU IGAKU (Jpn J Nucl Med)* 2005; 42: 1–10.
20. Graziano MJ, Henck JW, Meierhenry EF, Gough AW. Neurotoxicity of misonidazole in rats following intravenous administration. *Pharmacol Res* 1996; 33: 307–318.
21. Rajendran JG, Wilson DC, Conrad EU, Peterson LM, Bruckner JD, Rasey JS, et al. [(^{18})F]FMISO and [(^{18})F]FDG PET imaging in soft tissue sarcomas: correlation of hypoxia, metabolism and VEGF expression. *Eur J Nucl Med Mol Imaging* 2003; 30: 695–704.